Journal of Power Sources 252 (2014) 28–34

Contents lists available at ScienceDirect

Journal of Power Sources

journal homepage: www.elsevier.com/locate/jpowsour

Determination of lithium sulphur batteries internal resistance by the pulsed method during galvanostatic cycling☆

V.S. Kolosnitsyn, E.V. Kuzmina*, S.E. Mochalov

Laboratory of Electrochemistry, Institution of the Russian Academy of Sciences Institute of Organic Chemistry of Ufa Scientific Center of the Russian Academy of Sciences, 71, pr. Oktyabrya, Ufa 450054, Bashkortostan, Russia

HIGHLIGHTS

- The pulsed method as a way to determine the internal resistance of batteries.
- The internal resistance of Li–S cells depends on the depth of charge and discharge.
- The polarization direction of lithium sulphur cell governs the internal resistance.

ARTICLE INFO

Article history:
Received 9 September 2013
Received in revised form
18 November 2013
Accepted 20 November 2013
Available online 8 December 2013

Keywords:
Lithium sulphur cell
Impedance
Internal resistance
Direct Fourier transform
Pulsed method

ABSTRACT

The pulsed method of measuring impedance is described. The cell is galvanostatically stimulated by a bipolar current signal of square shape. The cell response is registered by sampling $U^{+}[i]$, $U^{-}[i]$ with selected period Δt. The impedance spectra are calculated by direct Fourier transform. The internal resistance of the lithium sulphur cell is characteristically minimum in the calculated impedance diagrams in the frequency range of 0.035–5 Hz. It is shown that the lithium sulphur cells have maximum internal resistance at the transient between high and low voltage plateaus of charge and discharge curves. The internal resistance increases significantly during the initial stages of cycling because of the formation of passivation layers at the electrodes. It was found that the internal resistance of the lithium sulphur cell in the same charge state is governed by the way in which it is achieved. This is explained by differences in molar volumes of products generated in the sulphur electrode by electrochemical reaction during charging and discharging.

1. Introduction

Internal resistance is one of the most important characteristics of accumulators because it limits their specific power and determines their thermal losses during charging and discharging. The internal resistance depends on the depth of charge (DoC) and depth of discharge (DoD) of the accumulators because the chemical composition and electro-physical properties of active electrode materials change during their charging and discharging. Therefore information on the dependence of internal resistance on DoD and/or DoC is necessary to design batteries. This is especially important for electric vehicles (EVs) and hybrid electric vehicles (HEVs).

DoD and DoC can significantly influence the internal resistance of cells with liquid cathodes. Unlike cells with electrolyte-insoluble active electrode materials (for example, lithium-ion or nickel–metal hydride cells), the chemical composition of the electrolyte and electrode are changing during the charging and discharging of cells with liquid cathodes (for example lithium sulphur cells). Therefore changes in the internal resistance of cells with liquid electrodes can be much greater than in cells with solid insoluble electrode materials.

The internal resistance can be measured by different methods. The calorimetric method of measuring the internal resistance is very attractive. According to this method the heat generated by the electrochemical cell under galvanostatic polarization is measured and the internal resistance is calculated by Joule's Law [1]. However, the application of this method is very complicated.

The methods of measuring the internal resistance on the basis of Ohm's Law are more acceptable. The applied signal (current or voltage) can be direct (DC), alternating (AC), or pulsed [3–5].

☆ This work was presented on the 224th ECS Meeting, Abstract #331, San Francisco, California, October 27–November 1, 2013.

* Corresponding author. Tel./fax: +7 (347) 2355800.
E-mail addresses: kolos@anrb.ru (V.S. Kolosnitsyn), kuzmina@anrb.ru, kuzmina.e.84@gmail.com (E.V. Kuzmina).

0378-7753/$ – see front matter © 2013 Elsevier B.V. All rights reserved.
http://dx.doi.org/10.1016/j.jpowsour.2013.11.099

Since the electrochemical cells have capacitive and inductive properties, their internal resistance is not only ohmic. Therefore DC methods are inapplicable for measuring the internal resistance of accumulators.

The AC methods are simple. Often the active resistance measured at a fixed frequency is accepted as internal resistance. Usually it is 1 kHz [2]. However this simple and universal approach cannot be correct for a variety of types of electrochemical systems and constructions. Since the frequency has a significant influence on the results, its selection is critical.

The measuring frequency must be low enough for the resistances of the electrolyte and the electrode reactions to be fully determined independently of the DoD/DoC of the cell. It should be noted that unreasonable decreases in frequency can significantly increase the measurement time.

The frequency of the measuring signal can be selected on the basis of cell impedance measured both at equilibrium and under polarization. However measuring and analyzing the impedance of a cell is a complex technical task.

The electrochemical impedance is measured separately for each frequency of the spectra. The measuring time increases when the frequency at which the measurement is made decreases. Therefore measurements of impedance in a wide range of frequencies, especially in the infra low frequency range, take a long time.

Moreover in that case it is possible to violate one of the basic hypotheses of the electrochemical impedance method – stationarity of the object [6]. The time of measuring the spectra must be minimal to secure the invariability of parameters of the electrochemical system. The impedance spectra can be obtained most quickly by the pulsed method [7].

The pulsed methods are widely used to measure the resistance of accumulators, for example VDA (Verband der Automobilindustrie, Frankfurt am Main, Germany) [3] and its modifications [5].

A rectangular current pulse with fixed duration and amplitude (current step methods) polarizes the cell. Then the response of the electrochemical system is recorded as changes of voltage and is analyzed in the time domain. There are some difficulties in nonlinear extrapolation of the curve of voltage changes at zero-time. In spite of that, as was shown in an overview [5], the value of internal resistance found by this method is close to the results of calorimetric measurements.

Elimination of these difficulties is possible by processing the results of similar experiments in the frequency domain. The voltage response to the current step stimulus is a step response. The impedance spectra can be computed by Fourier's transform of this response.

The aim of this work was to estimate the possibility of using the pulsed method with signal processing in the frequency domain to measure the internal resistance of the accumulator and to study changes in the internal resistance of the lithium sulphur cell during its continuous cycling.

2. Experiment

Estimation of the possibility of application of the pulsed method to measure the internal resistance of the cell was carried out using a laboratory prototype of the lithium sulphur cells.

2.1. Sample preparation

The sulphur electrode was made by dispersing 70 wt% sulphur (99.5%, Acros Organics), 10 wt% carbon black, and 20 wt% binder (PEO, Mw 4×10^6, Sigma–Aldrich) in acetonitrile (99.8%) to form a suspension. Then the suspension was coated onto carbon-coated aluminium foil. The coated electrodes were dried at 40 °C for 2 h, pressed by a twin-roller, and then cut into discs ($d = 28$ mm). The disc electrodes were dried in vacuum for 24 h at 60 °C.

Lithium foil (99.9%) with a thickness of 100 μm and a diameter of 25 mm was used as negative electrodes.

Electrolytes were made by dissolving lithium trifluoromethanesulfonate (CF_3SO_3Li, anhydrous, 99.9%, Sigma–Aldrich) in sulfolane (water content: 30–40 ppm).

Lithium sulphur cells were assembled by stacking the sulphur electrode, separator ($d = 28$ mm, Celgard 3501), and lithium metal electrode in stainless steel Swagelok® cells. Electrolyte preparation and cell assembly were carried out in a dry air atmosphere (water content ≤20 ppm).

2.2. Electrochemical measurements

The galvanostatic polarization and pulsed measurement of impedance were carried out by potentiostat, which was special designed and built in our laboratory [10]. The relative error of current stabilization was 0.1%. The voltage measurement error was 10 μV. The maximal sampling rate was 200 Hz.

The charge–discharge procedure was performed galvanostatically in a voltage range of 2.8–1.5 V at a charge current density of 0.1 mA cm^{-2} and discharge current density of 0.2 mA cm^{-2}. The experiments were carried out at 30 ± 0.1 °C.

Classical AC measurements of the impedance of the lithium sulphur cells were performed using a Solatron 1250 frequency response analyzer [8] and home-made potentiostat. The AC impedance was measured over a frequency range of 10 mHz–65 kHz with an excitation voltage of 10 mV and a resolution of 5 points per decade.

2.3. Electrochemical impedance spectroscopy by the pulsed method

The response of the system to the input action of arbitrary shape can be represented as a transfer function. It is a ratio of the Laplace transform of the output signal to the Laplace transform of the input signal. The corresponding Fourier transform is used to transit from a complex frequency to a real one:

$$H(j\omega) = \frac{F(y(t))}{F(x(t))} \tag{1}$$

Also the transfer function of system $H(j\omega)$ can be obtained from its step response $a(t)$ by direct Fourier transform [7]:

$$H(j\omega) = \int_0^\infty d/\mathrm{d}t(a(t))\exp(-j\omega t)\mathrm{d}t \tag{2}$$

where $a(t)$ is the step response or system response to step excitation.

In our investigations we stimulated the object with a current pulse with a square shape and then voltage changes of the object were registered [9,10]. If the input stimulus is the current and the step response is the voltage drop divided by applied current then the transfer function $H(j\omega)$ is the impedance. Then Equation (2) can be written as:

$$Z(j\omega) = a(0) + \int_0^\infty [(d/\mathrm{d}t)(a(t))]\exp(-j\omega t)\mathrm{d}t \tag{3}$$

where $a(0)$ is the initial drop of the step response and does not depend on frequency.

The experiment was carried out in the following way. At a selected moment the measuring bipolar current signal of square shape was added to the charge or discharge current (Fig. 1). This shape is similar to one full period of alternating current measurements and is preferable to a single unipolar pulse as the total amount of charge passed through the cell in one measurement is zero. The value of the applied current was selected such that the corresponding voltage amplitude was no more than 10 mV. The sample response was registered by sampling $U^+[i]$, $U^-[i]$ for a selected period Δt.

The resultant step response was generated from two half-periods of the response by averaging the respective sample:

$$a[i] = \left(\frac{U^+[i] - U_0^+}{\Delta I} + \frac{U^-[i] - U_0^-}{-2\Delta I}\right) \Big/ 2 \quad (4)$$

The integration of the Equation (3) is replaced by respective summing when the integration of the step response is given by sampling. In that case $a(0)$ is equal to $a[0]$.

Usually, the duration of the polarizing current and registration of the response is used as the upper limit of integration. More accurate results are obtained when the upper limit of integration has a value of $T = 1/2f = \pi/\omega$, which is governed by the frequency at which the impedance is calculated. This correlates to impedance calculation at the first harmonic. It is clear that the calculation algorithm based on the fast Fourier transform (FFT) is impossible in that case. However the direct Fourier transform (DFT) for any amount of points is not a problem with modern computational power.

The impedance spectrum was measured 10–30 times during charging or discharging. The step response was sampled in 15 ms, with a sampling rate of 500–4000 points per step response. The impedance spectra were calculated in the frequency range of 0.035–5 Hz with a resolution of 15 points per decade. Below it will be shown that the impedance fragment of the lithium sulphur cell of interest is located in this frequency range.

3. Results and discussion

There are two plateaus (~2.4 and ~2.2 V) in the charge–discharge curves of lithium sulphur cells (Fig. 2) corresponding to the electrochemical conversion of sulphur and lithium polysulphides. In the discharge process, sulphur initially electrochemically reduces to high ordered lithium polysulphide, for example to Li_2S_4 (Equation (5)), accompanied by active material transfer from solid phase to liquid. The high voltage plateau of the discharge curves corresponds to this process (Fig. 2a).

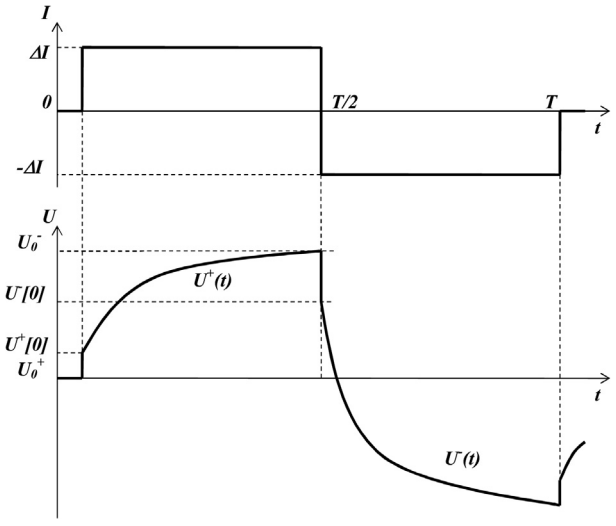

Fig. 1. $I(t)$ – applied signal, $U(t)$ – response signal.

$$S_8 + 4Li^+ + 4e^- \rightarrow 2Li_2S_4 \quad (5)$$

Then the generated lithium polysulphides reduce to lithium disulphide and lithium sulphide (Equation (6)), which are insoluble in the electrolyte. The active material transfers from liquid phase to solid during this step. The low voltage plateau of the discharge curve corresponds to this process (Fig. 2a).

$$Li_2S_4 + 2Li^+ + 2e^- \rightarrow Li_2S_2 + 2Li_2S \quad (6)$$

The reverse processes occur during the charging of lithium sulphur cells. Initially low ordered lithium polysulphides electrochemically oxidize to high ordered ones (Equation (7), low voltage plateau, Fig. 3b). This step is accompanied by active material transfer from solid phase to liquid.

$$2Li_2S_2 \rightarrow Li_2S_4 + 2Li^+ + 2e^- \quad (7)$$

At the beginning of the low voltage plateau, high ordered lithium polysulphide starts oxidizing to sulphur (Equation (8), Fig. 2b) and active material transfers from liquid phase to solid.

$$2Li_2S_4 \rightarrow S_8 + 4Li^+ + 4e^- \quad (8)$$

The impedance diagrams measured by the pulsed method are V-shaped independently of DoD or DoC (Fig. 2c, d). To interpret the impedances obtained by the pulsed method we measured the impedance spectra of a similar lithium sulphur cell by the AC method in a wide frequency range of 10 mHz–65 kHz (Fig. 3).

The shape of the AC impedance is typical for lithium sulphur cells [11–13] and is composed of a depressed semicircle at high frequencies and a short inclined line at low frequencies.

The high frequencies semicircle of the lithium sulphur cell is commonly related to the ohmic resistance and charge transfer resistance. The electrolyte resistance is determined by extrapolation of the impedance diagram to an infinitely large frequency. The low frequencies line is associated with diffusion within the cathodes.

Analysis of published papers shows that the shape of impedance diagrams of lithium sulphur cells does not practically depend on the chemical composition of the electrolyte [12,14–17] and positive electrodes [14,17–22], surface modifications of positive electrodes [23,24], binders [11,14,24], temperatures [25,26], and so on.

The single factor influencing the shape of the impedance diagram of lithium sulphur cells is the DoD/DoC [11–14,22,25]. The impedance diagrams of lithium sulphur cells discharged to 30–40% of DoD consist of a depressed semicircle and diffusion line [11–13]. The impedance diagrams have two depressed semicircles and a diffusion line for cells discharged to more than 30–40% of DoD [11–13,22]. It is important to notice that there is a characteristic minimum (V-shaped diagram) in the frequency range of 0.01–100 Hz between the semicircle and the diffusion line independently of the DoD/DoC of lithium sulphur cells. Thus, by comparing the impedance diagrams measured by the pulsed method (Fig. 2) and the classical AC method (Fig. 3), it follows that the sum of resistances of the electrolyte and electrode reactions of the lithium sulphur cell corresponds to the minimum position on the impedance diagram measured by the pulsed method.

Analysis of Fig. 3 and data described in Refs. [11–13,16] allows the following important conclusions to be drawn:

Firstly, the traditional frequency of 1 kHz at which internal resistance is measured corresponds to a random point on the

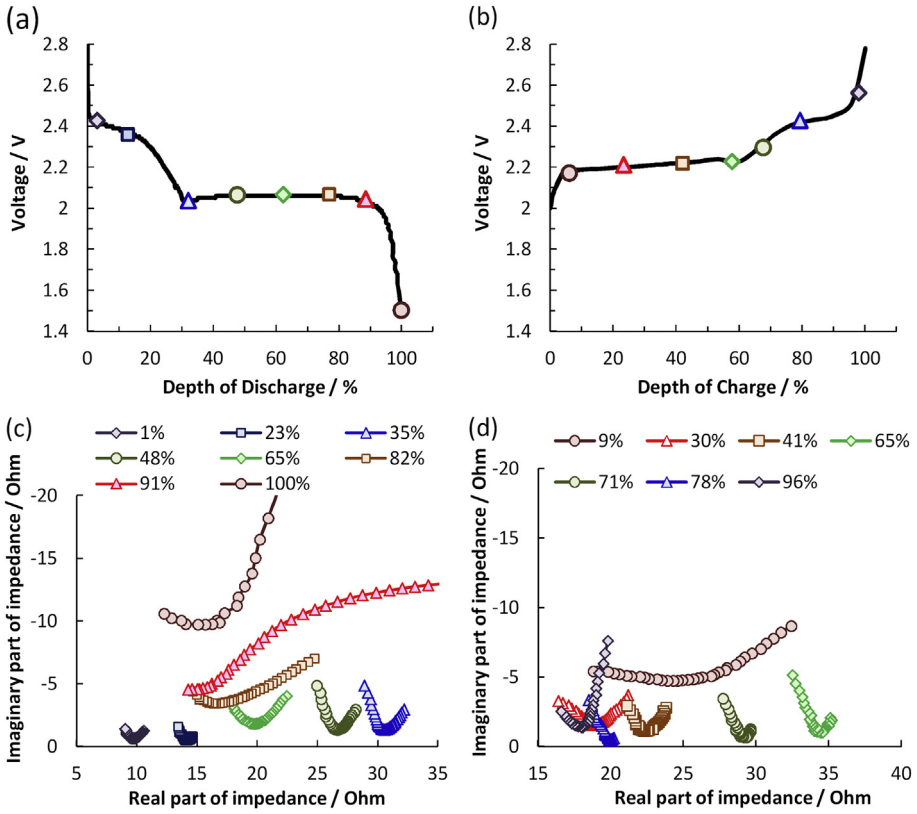

Fig. 2. Discharge (a) and charge (b) curves and impedance diagrams (c, d) in a frequency range of 0.035–5.0 Hz. The markers on the discharge and charge curves correspond to the presented impedance diagrams.

impedance diagram. This point is not the real internal resistance. The resistance measured at this frequency is much less than the sum of resistance of electrolyte and electrode. To properly estimate the internal resistance of lithium sulphur cells, the measurements must be done at much lower frequencies. Moreover the lowering of frequencies approximates the DC regime in which the cells are used in practice.

Secondly, the low frequencies part of the impedance is concentrated in a very narrow area of the impedance diagram. The impedance of cells weakly depends on the frequency in the range of 0.01–100 Hz. The measurements in this range give more reliable values of internal resistance and they appropriately describe cell behaviour under the direct current. We register this specific part of the impedance spectrum by the pulsed method. The impedance is practically ohmic in this frequency range and it can be considered as the internal resistance of cells.

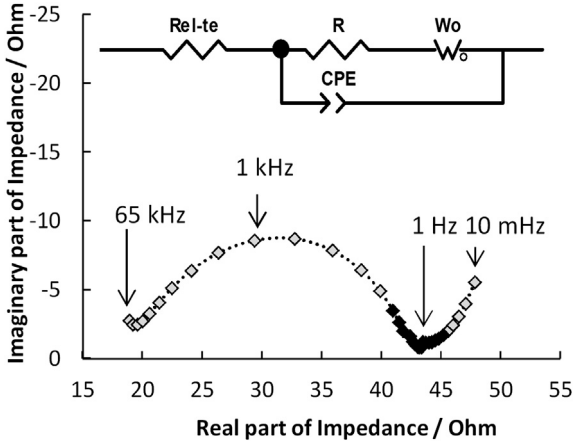

Fig. 3. Impedance diagram of non-polarized lithium sulphur cell in frequency range of 10 mHz–65 kHz. The range of 0.01–100 Hz is indicated by black dots.

Analysis of the obtained results shows that DoD influences the shape of the impedance diagrams obtained by the pulsed method (Fig. 2). The minimum of the impedance diagram is not sharp at high values of DoD (>80%) and is sharp at DoD < 80%.

It is known that during charging and discharging of lithium sulphur cells, the electrolyte and electrode change their composition [27–31]. When the cells are fully charged, electrolytes include a small amount of high ordered lithium polysulphides and there is sulphur in the macro-pores of sulphur electrodes and in the micro- and meso-pores of carbon contained in the electrodes. The impedance diagram of a fully charged lithium sulphur cell is a V-shaped curve whose minimum defines the internal resistance of the cell (Fig. 2c).

While the cell is discharging, the V-shaped impedance diagram is continuously broadening and the minimum is shifting to the range of larger values of resistance. These changes of shape and position of the impedance diagram reflect the changes in the properties of the electrolyte and electrodes of lithium sulphur cells.

As mentioned above, during the initial stage of discharge of lithium sulphur cells (DoD < 30%), sulphur reduces to high ordered lithium polysulphides, which dissolve in electrolyte solutions, increasing the viscosity of the electrolyte and decreasing its conductivity.

The shifting of impedance to the range of larger values of resistance is explained by the decreasing of the electrolyte conductivity. The broadening of the impedance diagram of the lithium sulphur cell is likely to be related to changes in the transport properties of electrolytes, which cause a decrease in the charge transfer rate and diffusion limitations inside the sulphur electrodes.

After sulphur has reduced to middle ordered lithium polysulphide (Li_2S_n, $n = 3–4$), the sulphur contained in the lithium polysulphides starts to reduce (low voltage plateau) to lithium disulphide and lithium sulphide. Lithium sulphide is insoluble in the electrolytes and therefore it deposits in the pores of the sulphur electrode and on the surface of carbon particles. The concentration of lithium polysulphides decreases in the electrolyte and its conductivity increases.

The changes in the composition of the electrolyte and sulphur electrode are reflected on the impedance diagram. The impedance diagram shifts to lower values of resistance during the discharge of the lithium sulphur cell at the low voltage plateau. This shift is caused by increases in the conductivity of the electrolyte because of reduction of the lithium polysulphide. The broadening of the impedance diagram reflects the degradation transport properties of the sulphur electrode and carbon–electrolyte border because of lithium sulphide precipitation.

During charging there are similar changes in the impedance diagram of lithium sulphur cells in reverse order.

To illustrate the possibility use of the described method for the diagnosis of the state of lithium sulphur cells, the dependences of internal resistance on DoD/DoC are shown in Fig. 4. The internal resistance was calculated at the minimum of the imaginary part of the impedance diagram. Similar dependences were obtained for AC impedance in papers [11–13] for lithium sulphur cells with different compositions of electrolyte and sulphur electrodes.

The maximum of internal resistance repeats from cycle to cycle during all charge–discharge cycling and correlates with the DoD and DoC in which the concentration of lithium polysulphides is maximal in the electrolyte. Also it should be noted that the internal resistance of lithium sulphur cells is greater in the high voltage plateau state than in the low voltage plateau state. This shows the greater constant rate of electrochemical oxidization and reduction of sulphur compared to lithium polysulphides.

The lithium sulphur cells are characterized by the relative large capacity fade and changes of internal resistance (Fig. 5) during long-duration cycling [32–34]. The internal resistances measured in one charge state are changing differently for charging (Fig. 5a) and discharging (Fig. 5b) during long-term cycling.

3.1. The internal resistance of lithium sulphur cells measured at charging

The capacity decreases by 0.7–1.5% per cycle (Fig. 5c) and the internal resistance increases 1.2–1.4 (Fig. 5a) times relative to the first cycle during the first 15–20 cycles. At the same time, the efficiency of cycling decreases and stabilizes at a level of 86–90% (Fig. 5d).

The initial increase in internal resistance is likely to be caused by the formation of passive layer on the lithium electrodes and redistribution of active components in the sulphur electrode volume.

After 15–20 cycles the rate of capacity fade is stabilized and is about 0.2–0.4% per cycle relative to the discharge capacity of the first

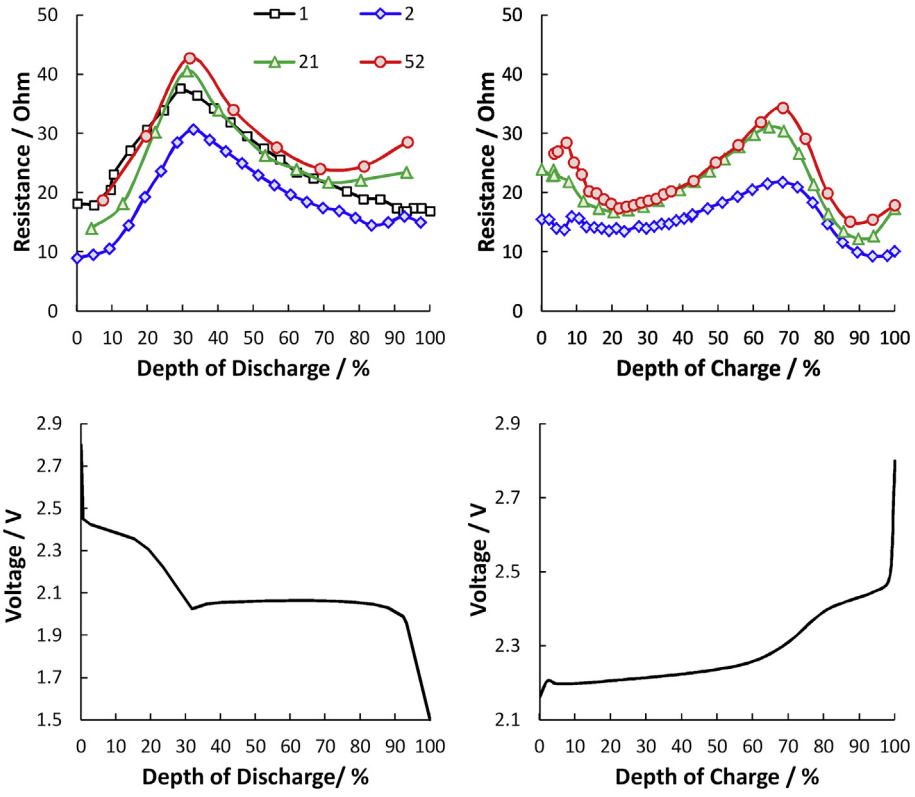

Fig. 4. The dependences of internal resistance on the depth of discharge (DoD) and depth of charge (DoC) of the lithium sulphur cell. The cycle numbers are given in the legend.

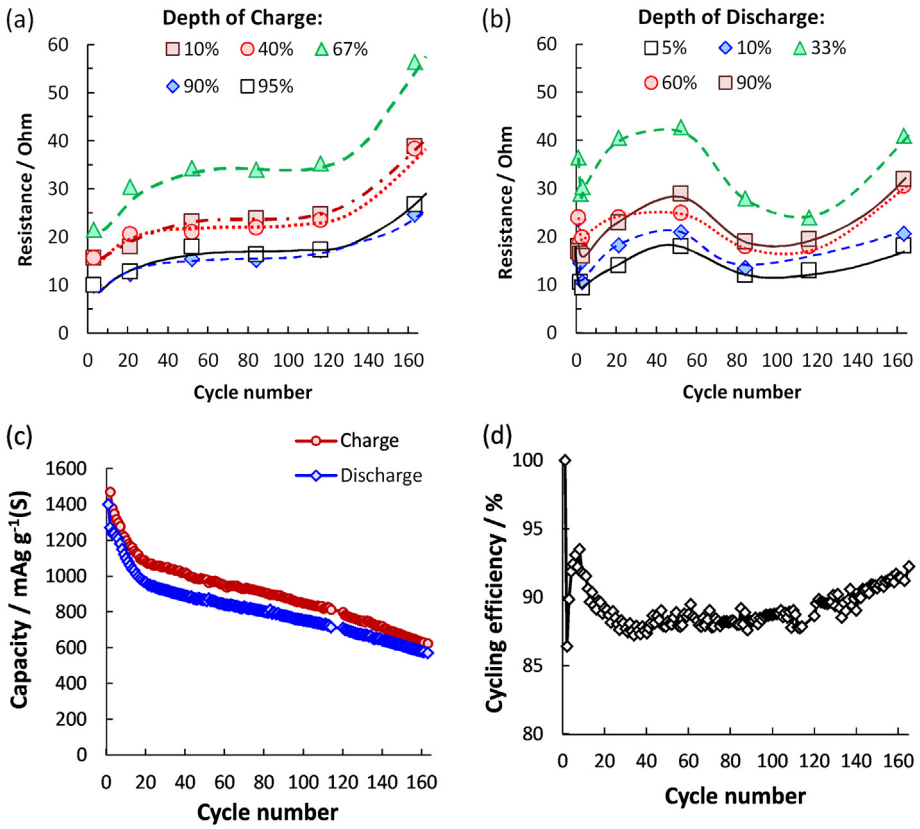

Fig. 5. The dependences of the internal resistance measured during charging (a) and discharging (b) on the cycle number and cycle performance (c, d) of the lithium sulphur cell. DoD and DoC are given in the legends.

cycle. The rate of increase in internal resistance is about 0.02–0.05 Ω per cycle. After the 100th cycle, the internal resistance measured during charging continues to increase at an average rate of 0.3–0.6 Ω per cycle.

3.2. *The internal resistance of lithium sulphur cells measured at discharging*

The internal resistance measured at discharging changes in a complicated manner during cycling (Fig. 5b). The internal resistance measured at 1st cycle is greater than measured at 2nd cycle. For the next 60 cycles the internal resistance measured at discharging increases with average rate of 0.2–0.6 Ω per cycle. Then the internal resistance decreases until the 120th cycle. From the 120th cycle the internal resistance increases again.

We believe that differences in the changes in internal resistance during charging and discharging and dynamics of these changes may be caused by differences in the properties of solid products of charging and discharging.

The lithium sulphide is generated at the surface of carbon particles of sulphur electrode at discharging (Equation (8)) and elemental sulphur is generated at charging (Equation (6)). The densities and consequently molar volumes[1] of lithium sulphide and sulphur are dramatically different. The density and the molar volume of sulphur is 2.07 g cm^{-3} [35] and 15.5 cm^3 mol^{-1}, respectively. The density and the molar volume of lithium sulphide is 1.64 g cm^{-3} [35] and 28.0 cm^3 mol^{-1}, respectively. Science the molar volume of lithium sulphide is significantly greater than one of sulphur during the discharging the thickness of sulphur electrode is increasing. Therefore the internal resistance is increasing. The increasing of thickness of positive electrodes at discharging and decreasing its at charging are shown in paper [36].

During cycling of lithium sulphur cells the electrochemical active surface of positive electrode is decreasing due to irreversible passivation of carbon particles by Li_2S, Li_2S_2 and products of destruction of electrolyte as well as violations of electronic contacts of the carbon particles with current collector [37–39]. The internal resistance gradually increases during cycling.

The passivation of positive electrode by sulphur and lithium sulphide (the electrochemical products, Equations (6) and (8)) strongly effects on the properties of the positive electrode after continuous cycling. Elemental sulphur is generated during charging and passivates the electrode less because of its smaller molar volume. Therefore the properties of the charged electrode change insignificantly during continuous cycling.

4. Conclusions

It was shown that the internal resistance of lithium sulphur cells could be measured by the characteristic minimum of the impedance diagram in the frequency range of 0.035–5 Hz obtained by the pulsed method with a galvanostatic stimulus.

It was estimated that the impedance of a lithium sulphur cell does not depend significantly on frequency in the range of 0.035–5 Hz; it is ohmic and corresponds to the sum of resistances of electrode reactions and electrolytes.

The dependence of internal resistance on DoD and DoC was studied by the proposed method. It was shown that the internal resistance of the lithium sulphur cell is maximal at the transition

[1] The molar volume is calculated as ratio of molar weight and density.

from the high voltage plateau to the low voltage plateau of the charge and discharge curves. A significant increase in internal resistance occurs in the initial stages of cycling.

It was found that in the same charge state the internal resistance of the lithium sulphur cell is governed by the way in which it is achieved. This is caused by the different properties of the product generated in the sulphur electrode by electrochemical reaction during charging and discharging. Sulphur is formed during charging and has a smaller molar volume ($V_m(S) = 15.5\ cm^3\ mol^{-1}$) than lithium sulphide ($V_m(Li_2S) = 28.0\ cm^3\ mol^{-1}$) generated during discharging.

References

[1] Y. Kobayashi, H. Miyashiro, K. Kumai, K. Takei, T. Iwahori, I. Uchida, J. Electrochem. Soc. 149 (2002) A978–A982.
[2] URL: http://www.maccor.com/series4000.php.
[3] URL: http://www.vda.de.
[4] G.G. Min, Y. Ko, T.-H. Kim, H.-K. Song, S.B. Kim, S.-M. Park, J. Electrochem. Soc. 158 (2011) A1267–A1274.
[5] H.-G. Schweiger, O. Obeidi, O. Komesker, A. Raschke, M. Schiemann, C. Zehner, M. Gehnen, M. Keller, P. Birke, Sensors 10 (2010) 5601–5625.
[6] E. Barsoukov, J.R. Macdonald, Impedance Spectroscopy Theory, Experiment, and Applications, second ed., Wiley Interscience, New Jersey, 2005, p. 595.
[7] S. Goldman, Transformation Calculus and Electrical Transients, Prentice-Hall, New York, 1949, p. 439.
[8] URL: http://www.solartronanalytical.com/.
[9] E. Barsoukov, S.H. Ryu, H. Lee, J. Electroanal. Chem. 536 (2002) 109–122.
[10] S.E. Mochalov, V.S. Kolosnitsyn, Instrum. Exp. Tech. 23 (2000) 53–55.
[11] L. Yuan, X. Qiu, L. Chen, W. Zhu, J. Power Sources 189 (2009) 127–132.
[12] W. Ahn, K.-N. Kim, K.-N. Jung, K.-H. Shin, C.-S. Jin, J. Power Sources 202 (2012) 394–399.
[13] V.S. Kolosnitsyn, E.V. Kuzmina, E.V. Karaseva, S.E. Mochalov, J. Power Sources 196 (2011) 1478–1482.
[14] J.-W. Choi, J.-K. Kim, G. Cheruvally, J.-H. Ahna, H.-J. Ahn, K.-W. Kim, Electrochim. Acta 52 (2007) 2075–2082.
[15] W. Zheng, Y.W. Liu, X.G. Hua, C.F. Zhang, Electrochim. Acta 51 (2006) 1330–1335.
[16] M. Rao, X. Geng, X. Li, S. Hua, W. Li, J. Power Sources 212 (2012) 179–185.
[17] J. Wang, J. Chen, K. Konstantinov, L. Zhao, S.H. Ng, G.X. Wang, Z.P. Guo, H.K. Liu, Electrochim. Acta 51 (2006) 4634–4638.
[18] B. Zhang, B.C. Lai, Z. Zhou, X.P. Gao, Electrochim. Acta 54 (2009) 3708–3713.
[19] J.-J. Chen, X. Jia, Q.-J. She, C. Wang, Q. Zhang, M.-S. Zheng, Q.-F. Dong, Electrochim. Acta 55 (2010) 8062–8066.
[20] L. Yuan, H. Yuan, X. Qiu, L. Chen, W. Zhu, J. Power Sources 189 (2009) 1141–1146.
[21] J.-Z. Wang, L. Lu, M. Choucairc, J.A. Stride, X. Xu, H.-K. Liu, J. Power Sources 196 (2011) 7030–7034.
[22] M. Rao, X. Song, E.J. Cairns, J. Power Sources 205 (2012) 474–478.
[23] J. Hassoun, M. Agostini, A. Latini, S. Panero, Y.-K. Sun, B. Scrosati, J. Electrochem. Soc. 159 (2012) A390–A395.
[24] Y.-J. Choi, Y.-D. Chung, C.-Y. Baek, K.-W. Kim, H.-J. Ahn, J.-H. Ahn, J. Power Sources 184 (2008) 548–552.
[25] X. Liang, Z. Wen, Y. Liu, H. Zhang, L. Huang, J. Jin, J. Power Sources 196 (2011) 3655–3658.
[26] H.-S. Ryu, H.-J. Ahn, K.-W. Kim, J.-H. Ahn, K.-K. Cho, T.-H. Nam, J.-U. Kim, G.-B. Cho, J. Power Sources 163 (2006) 201–206.
[27] R. Dominiko, R. Demir-Cakan, M. Morcrette, J.-M. Tarascon, Electrochem. Commun. 13 (2011) 117–120.
[28] K. Kumaresa, Y. Mikhaylik, R.E. White, J. Electrochem. Soc. 155 (2008) A576–A582.
[29] Y. Diao, K. Xie, S. Xiong, X. Hong, J. Electrochem. Soc. 159 (2012) A421–A425.
[30] M. Hagen, P. Schiffels, M. Hammer, S. Dörfler, J. Tübke, M.J. Hoffmann, H. Althue, S. Kaskelc, J. Electrochem. Soc. 160 (2013) A1205–A1214.
[31] Y. Li, H. Zhan, S. Liu, K. Huang, Y. Zhou, J. Power Sources 195 (2010) 2945–2949.
[32] V.S. Kolosnitsyn, E.V. Karaseva, Russ. J. Electrochem. 44 (2008) 506–509.
[33] S.S. Zhang, J. Power Sources 231 (2013) 153–162.
[34] Z. Deng, Z. Zhang, Y. Lai, J. Liu, J. Li, Y. Liu, J. Electrochem. Soc. 160 (2013) A553–A558.
[35] Physical Constants of Inorganic Compounds, in: David R. Lide (Ed.), CRC Handbook of Chemistry and Physics, 90th Edition (CD-ROM Version, CRC Press/Taylor and Francis, Boca Raton, FL, 2010.
[36] X. He, J. Ren, L. Wang, W. Pu, C. Jiang, C. Wan, J. Power Sources 190 (2009) 154–156.
[37] R. Elazari, G. Salitra, Y. Talyosef, J. Grinblat, C. Scordilis-Kelley, A. Xiao, J. Affinito, D. Aurbach, J. Electrochem. Soc. 157 (2010) A1131–A1138.
[38] S.E. Cheon, S.S. Choi, J.S. Han, Y.S. Choi, B.H. Jung, H.S. Lim, J. Electrochem. Soc. 151 (2004) A2067–A2073.
[39] Y. Diao, K. Xie, S. Xiong, X. Hong, J. Electrochem. Soc. 159 (2012) A1816–A1821.